CURTAILMENT OF WIND FARM POWER OUTPUT THROUGH FLEXIBLE TURBINE OPERATION USING WIND FARM CONTROL

Sung-ho Hur and William E. Leithead
Department of Electronic and Electrical Engineering
University of Strathclyde
sung.h.hur@strath.ac.uk

Abstract:

When the installed capacity of wind power becomes high, the power generated by wind farms can no longer simply be that dictated by the wind speed. With sufficiently high penetration, it will be necessary for wind farms to provide assistance with supply-demand matching. The work presented here introduces a wind farm controller that regulates the power generated by the wind farm to match the grid requirements by causing the power generated by each turbine to be adjusted. Further benefits include fast response to reach the wind farm power demanded, high accuracy, little variability in the wind farm power output and provision of synthetic inertia.

Keywords: Wind farm power control, wind turbine control, flexible turbine operation.

1 Introduction

When the installed capacity of wind power becomes high, the power generated by wind farms can no longer simply be that dictated by the wind speed. Already, the operation of some wind turbines is being curtailed. With sufficiently high penetration, it will be necessary for wind farms to provide services to the grid including spinning reserve, frequency support and assistance with supply-demand matching. In these circumstances, to regulate the power generated by the wind farm to match the grid requirements, a wind farm controller, causing the power generated by each turbine to be adjusted, is required.

The structure of the wind farm controller discussed here is shown in Figure 1. It has two elements, the Network Wind Farm Controller (NWFC) and the Turbine Wind Farm Controller (TWFC). The NWFC acts on information regarding the state of the power network to determine the required power output from the wind farm and so the adjustment (ΔP) relative to P, the wind speed dictated output that would arise with no adjustment. The TWFC acts on information regarding the state of the wind farm and the turbines therein to allocate adjustments to each turbine, ΔP_i (for $i = 1, \dots, N$, where N is the number of turbines in the farm) relative to P_i, the wind speed dictated output of turbine i.

Each wind turbine in the farm has its own full operational envelope controller [1] that ensures the wind turbine follows its required operating strategy and remains in a safe operating condition through regulating rotor speed, torque and some loads. Since the wind farm controller requires each turbine to adjust its power output on request, the full envelope controller is modified by addition of a Power Adjusting Controller (PAC) [2]. The PAC causes the turbine to adjust its generated power by a demanded amount relative to that dictated by the wind speed. As the PAC is essentially a feed forward controller, jacketing the full envelope controller, it does not compromise the operation of the full envelope controller, hence redesigning or retuning of the existing full envelope controller is not necessary. Furthermore, the PAC contains safeguards to prevent the turbine being driven into unsafe operating regions. The PAC is sufficiently fast acting to provide the turbine with a synthetic inertia response [3].

To prevent the introduction of feedback loops between the wind farm controller and the individual turbines as depicted in Figure 1, the only communication regarding the state of each turbine to the wind farm controller is through flags, f_i. Furthermore, since the wind farm consists of a large number of turbines, the wind farm controller feedback acting on the total power output from the farm only introduces very weak feedback on each turbine. In other words, as the number of turbines that share the adjustments to the wind farm power output increases, the feedback effect decreases. Hence, the wind farm controller acts independently to the controllers of the wind turbines.

The purpose of this paper is to investigate the design and performance of the wind farm controller in Figure 1 with the objective of operating the wind farm at some specified output power. The controller not only adjusts the total power generated but allocates the individual adjustments to each turbine.

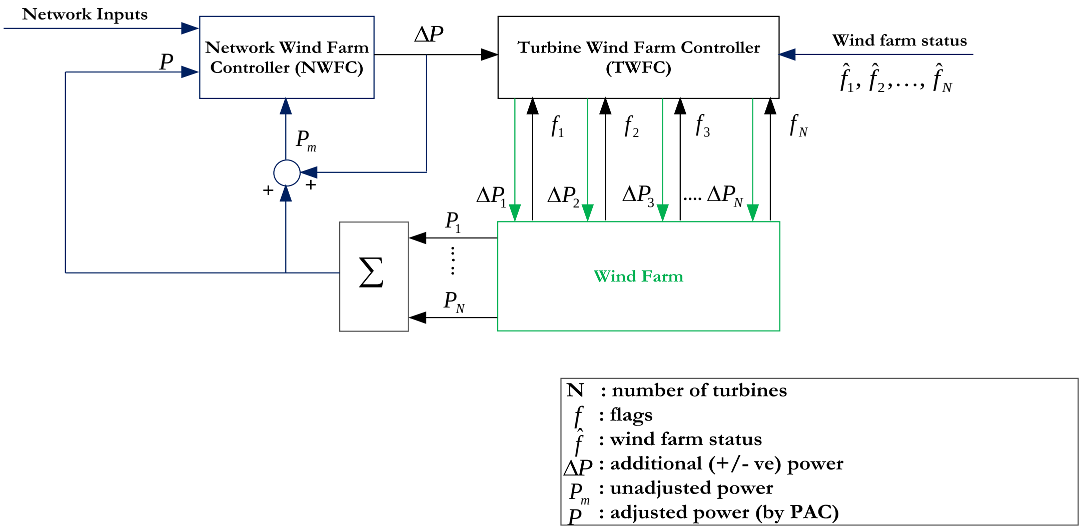

Figure 1: Structure of the wind farm controller.

The design of the wind farm controller is presented in Section 2. Its performance is presented in Section 3 by being applied to curtail the power output of a 10 turbine wind farm. The wind farm is modelled using both Matlab/SIMULINK and BLADED. The turbines are the Supergen (Sustainable Power Generation and Supply) Wind 5MW wind turbine. Conclusions are drawn in Section 4.

2 Wind Farm Control

The wind farm controller requires that each variable-speed pitch-regulated wind turbine be equipped with an existing central (full envelope) controller and PAC. The central controller causes the turbine to track its design operating curve as depicted in Figure 2; that is, a constant generator speed (i.e., 70 rad/s) is maintained in the lowest wind speeds (mode 1); the C_{pmax} curve is tracked to maximise the aerodynamic efficiency in intermediate wind speeds (mode 2); constant generator speed (i.e., 120 rad/s) is again maintained in higher wind speeds (mode 3); and above rated wind speed, the rated power of 5MW is maintained by active pitching (mode 4) [4], [5].

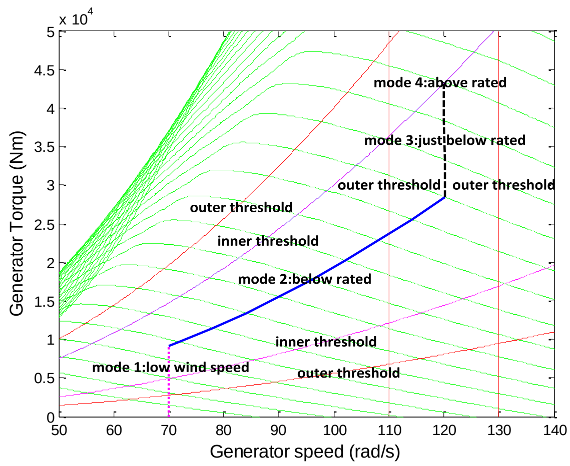

Figure 2: Design operating curve over the full envelope operation and the thresholds for the wind farm control strategy.

The PAC provides fully flexible operation adjusting the power output from each turbine, more specifically, reducing the power or increasing the power for a limited time if required. However, if an increase or decrease in the power output is sustained, the turbine operating state could move away from the design operating curve.

The wind farm controller regulates the wind farm power output ensuring, at the same time, that each turbine (with the central controller and PAC) operates within the safe operating region defined by the thresholds in Figure 2. In below rated wind speed, the turbines operating inside the inner thresholds could be allocated greater adjustments in power than the turbines operating outside the inner thresholds. The turbines operating outside the outer thresholds will be allocated zero adjustment in power to bring them back onto the design operating curve. The same strategy is applied in modes 3 and 4 except that there are no inner bounds since the deviation from the design operating curve caused by the PAC in above rated wind speed is smaller than the deviation in below rated wind speed.

In this paper, it is assumed that every turbine has the same status except that they operate in different wind speeds. The wind is stochastically varying with time and continuously interacting with the rotor. The effective wind speed is wind speed averaged over the rotor area such that the spectrum of aerodynamic torque remains unchanged. It is obtained by filtering the point wind speed [6] through the filter introduced in [7]. The point wind speeds that take into account the correlation of layout of the cluster is obtained from BLADED.

Different wind speeds cause the turbines to operate on different parts of the design operating curve (Figure 2). The wind farm controller adjusts the power for each turbine based on its status with reference to the inner and outer thresholds. The thresholds are determined on the generator torque (T_e) vs generator speed (ω_g) plane since the central controller is designed to follow the design strategy curve on the T_e vs ω_g plane although some other existing controllers are designed to follow the design strategy curve on the aerodynamic torque (T_f) vs rotor speed (Ω) plane [8], in which case the thresholds would be determined on the T_f vs Ω plane. Each threshold is defined as

$$y_T = T_e - k_T \omega_g^2 \quad (1)$$

where k_T is a constant, unique for each threshold. For instance, for the outer threshold above the C_{pmax} curve, y_T becoming positive indicates that the threshold has been crossed. Hysteresis loops are incorporated into the thresholds to avoid chattering. The hysteresis limit in the direction outwards from the C_{pmax} curve is set to 10^3, while the limit in the direction towards the C_{pmax} curve is set 5 times larger since it tends to move more rapidly when moving towards the C_{pmax} curve.

In mathematical terms, ΔP is computed as

$$\Delta P(t) = k_i \int P_d(t) - P_d(t) dt \tag{2}$$

where $\Delta P(t)$ and $P_d(t)$ denote adjusted power and the demanded power, respectively, and k_i is a tuning parameter.

Consequently, unadjusted power, P_m (the wind speed dictated wind farm power output that would arise with no adjustment) would be

$$P_m = P - \Delta P \tag{3}$$

When ΔP is negative, the TWFC distributes ΔP to each turbine as ΔP_i based on flags, f_i (status of each turbine) and $\hat{f}_i$ (wind farm status as depicted in Figure 1) as follows

$$\Delta P_i = \frac{\Delta P \min(f_i - \hat{f}_i)}{\sum_{i=1}^{N_T} \min(f_i - \hat{f}_i)} \tag{4}$$

for $i = 0,1,\ldots,N_T$. The implication is that

$$\sum_{i=1}^{N_T} \Delta P_i = \Delta P \tag{5}$$

where N_T denotes the number of turbines in the wind farm.

In mode 2, flags are returned as 0, 1 or f_m, which is 3 in this paper. If a turbine is operating within the inner threshold (Figure 2), a flag of f_m would be returned. If a turbine is operating within the outer threshold but outside the inner threshold, a flag of 1 would be returned. Finally, if a turbine is operating outside the outer threshold, a flag of 0 would be returned. ΔP_i with a flag of 0 would be zero, and ΔP_i with a flag of 3 would be 3 times larger than ΔP_i with a flag of 1. These numbers are design parameters that can be altered appropriately. In modes 3 and 4, only the outer thresholds exist and, thus, only flags of 0 and f_m are present.

The wind farm status could be determined by a number of factors including the health, age and location of the turbines. For instance, reduction in generated power may be made to only half the wind turbines in the farm, those on the up-wind side of the farm [2]. The wind farm status, $\hat{f}_i$ (for $i = 0,1,\ldots,N_T$) is also returned as 0, 1 or f_m in mode 2 and 0 or f_m in modes 3 and 4. In turn, $\hat{f}_i$ and f_i are compared and the minimum is utilised in (4). However, as previously mentioned, it is assumed that every turbine has the same status in this paper; that is, $\hat{f}_i = f_m$ (for all i).

When ΔP is positive, the change in ΔP_i impacts on the turbine operating state much more significantly, causing turbines to cross the outer threshold more readily. Thus, (4) and (5) need to be modified as follow. More detailed justification for the following modification is presented with a simulation example in Section 3.2.

$$\Delta P_i = Q_i \frac{\Delta P \min(f_i - \hat{f}_i)}{\sum_{i=1}^{N_T} \min(f_i - \hat{f}_i)} \tag{6}$$

where

$$Q_i = \frac{\sum_{i=1}^{N_T} f_i}{N_T f_m} \tag{7}$$

and (5) is subsequently replaced with

$$\sum_{i=1}^{N_T} \Delta P_i \neq \Delta P \tag{8}$$

only if ΔP is positive.

The allocation and reallocation of the power adjustment should take place in a smooth manner, which avoids the introduction of large transients, discontinuities and steps in the wind farm power output. It is achieved by filtering f_i (for $i = 0,1,\ldots,N_T$) to ensure that the smoothing occurs only when the switching takes place; that is, filtering f_i is equivalent to filtering ΔP_i only when the switching takes place. A low pass filter, with time constant of 3 s, is exploited although it could be larger in real life.

The central controller ensures that the switching between the various modes (Figure 2) also takes place in a smooth manner. In mode 1, the PAC is not activated.

3 Simulation results

Matlab/Simulink and BLADED models of the Supergen 5MW exemplar turbine are used. The rated wind speed is approximately 11.5 m/s. The BLADED model provides greater details for the structural loads, while the Matlab/Simulink model enables many turbines to be included in a wind farm model. The wind farm model thus consists of 9 Matlab/Simulink models and 1 BLADED model. The two software packages are connected using StrathControl Gateway, a commercial software package that fully integrates the simulation. Due to the high computational demand, it is assumed that the wind farm contains only 10 turbines.

A number of simulations have been conducted to demonstrate how the wind farm control strategy performs, and three of these simulations are reported in this section. In Simulation 1, ΔP is always negative in below rated wind speed. In Simulation 2, ΔP alternates between negative and positive in below rated wind speed. In Simulation 3, ΔP is always negative in just below rated wind speed that requires the central controllers to switch between modes 2 and 3.

The frequency analysis for examining the feedback (as depicted in Figure 1) effect that could adversely affect the performance of the full envelope controllers is also discussed for Simulation 3.

3.1 Simulation 1

In Simulation 1, the wind farm is required to produce a constant power of 12 MW at a mean wind speed of 8 m/s. Adjusted power in blue is depicted against unadjusted power in red in Figure 3. The PAC is switched on at 120 s past the transient response, and ΔP always remains negative.

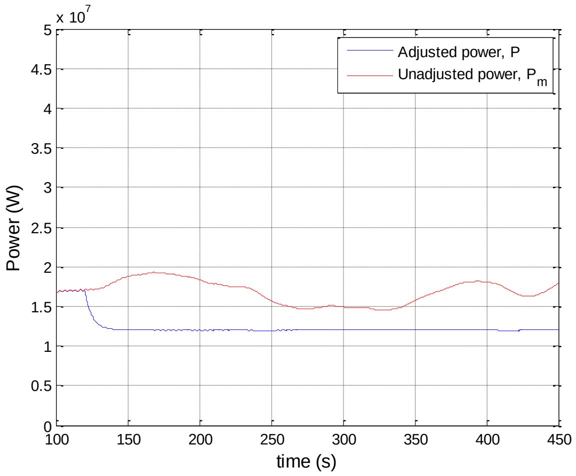

Figure 3: Simulation 1: adjusted vs unadjusted power.

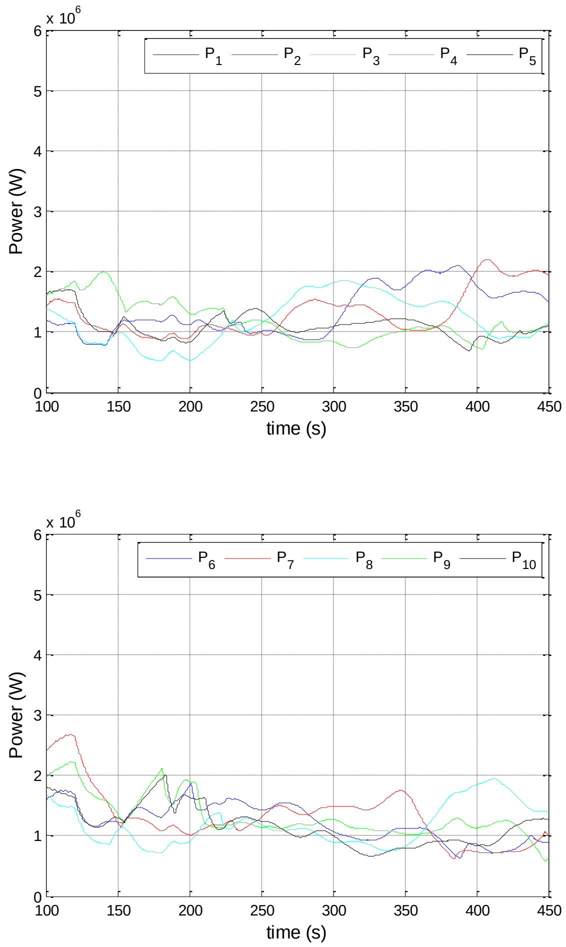

Figure 4: Simulation 1: power outputs from each turbine.

Since it is the wind farm power output that is regulated, the individual power output from each turbine is still changing and being adjusted as depicted in Figure 4. The turbines experiencing lower wind speeds, for much of the time, generate less than 1.2 MW (demanded power output divided by the number of turbines, N), whilst those experiencing higher wind speeds, for much of the time, generate more than 1.2 MW. In total, a constant wind farm power output of 12 MW is produced as depicted in blue in Figure 3.

In the same situation, if the turbines were curtailed individually to 1.2 MW (subsequently adding the individual power outputs together to yield the wind farm power output), the individual power outputs would be reduced below 1.2 MW when some turbines experience lower wind speeds as depicted in Figure 5. Consequently, as depicted in Figure 6, the output from the wind farm would, for much of the time, be less than 12 MW as depicted in red against the adjusted power by the wind farm controller.

In summary, with the wind farm control strategy introduced here, by curtailing the wind farm power output in place of the individual wind turbine power outputs, the turbines seeing higher wind speeds compensate those seeing lower wind speeds, producing an improved result as depicted in Figure 6. Another benefit of curtailing the wind farm power output rather than the individual power outputs is that it does not necessitate redesigning or retuning of the existing central controllers; that is, incorporating PAC into the existing central controller does not alter the dynamics of the central controller as discussed in more detail in Section 3.3.

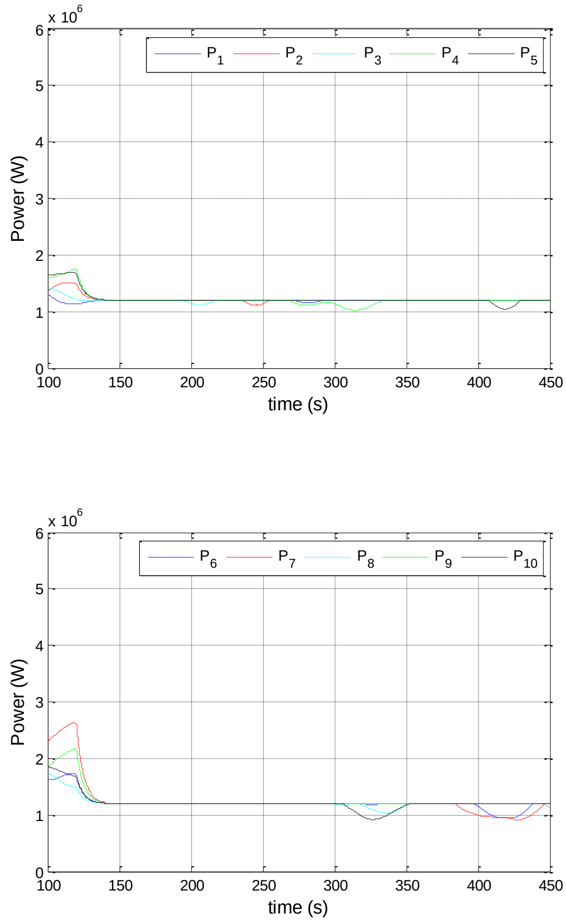

Figure 5: Individual curtailment: curtailed power outputs from each turbine.

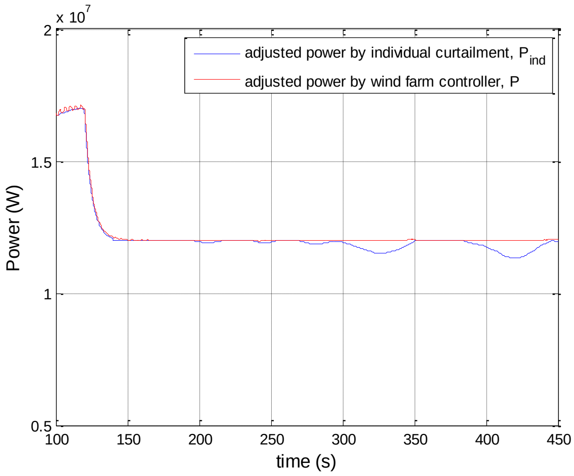

Figure 6: Adjusted power by individual curtailment vs adjusted power by the wind farm control strategy.

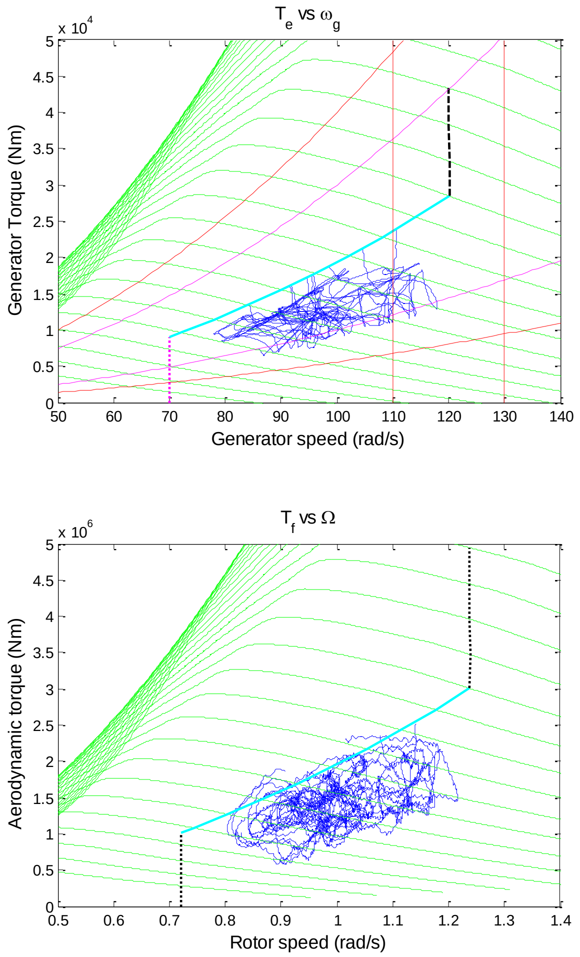

Figure 7: Simulation 1: Behaviour of each turbine on the generator torque and generator speed plane (upper subfigure) and the aerodynamic torque and rotor speed plane (lower subfigure).

The behaviour of each turbine on the T_e vs ω_g plane and the T_f vs Ω plane [8] is also depicted in Figure 7. As reported in Section 2, the strategy is based on the T_e vs ω_g plane; that is, thresholds are designed on this plane. The results demonstrate that the turbines operate within the inner thresholds, allowing for the hysteresis loops. In more detail, when a turbine crosses the inner threshold, the turbine is allocated smaller adjustment in power, as the flag changes from 3 to 1, thereby causing the turbine either to slow down in moving outwards from the design operating curve or to move towards the design operating curve. In this example, setting the flags to 1 from 3 diverts the turbine towards the design operating curve, and the outer threshold is never reached.

Despite all the allocation and reallocation of ΔP to each turbine as illustrated in Figures 4 and 7, a constant power of 12 MW is still maintained with little variability as depicted in Figure 3.

3.2 Simulation 2

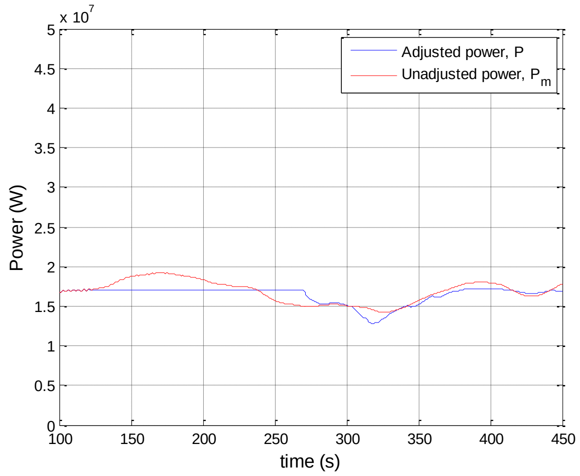

Figure 8: Simulation 2: adjusted power vs unadjusted power.

In Simulation 2, the wind farm is required to produce a constant power of 18MW at a mean wind speed of 8 m/s. Adjusted power in blue is depicted against unadjusted power in red in Figure 8. The PAC is switched on at 120 s past the transient response. It depicts that ΔP alternates between positive and negative. Though P can be held smaller than P_m ($\Delta P < 0$) persistently, P cannot be held larger than P_m ($\Delta P > 0$) indefinitely. Moreover, positive ΔP must be compensated afterwards [2]. Consequently, P drops at around 270s, and ΔP remains negative from around 270 until it is fully compensated.

The behaviour of each turbine on the T_e vs ω_g plane and the T_f vs Ω plane is also depicted in Figure 9. When turbines cross the inner threshold, the turbines are allocated smaller ΔP_i (as the flags change from 3 to 1). It diverts some turbines towards the design operating curve, but some turbines still move towards the outer threshold, but more slowly now, in contrast to Simulation 1, where changing the flags from 3 to 1 diverts each turbine towards the design operating curve. When the turbines eventually cross the outer threshold, the flags change from 1 to 0, finally redirecting them towards the design operating curve as illustrated in Figure 9. During this so-called recovery process, the previous positive ΔP_i is compensated.

In this simulation, where ΔP is positive, if (4) were still exploited instead of (6), the remaining turbines would compensate for the turbines that have crossed the outer threshold, thereby satisfying (5). For instance, when turbine 1 crosses the outer threshold above the design operating curve, ΔP_1 would become zero to bring turbine 1 back to the design operating curve (leaving the turbine in the recovery process), and ΔP_i of the remaining turbines would increase to compensate and, thus, satifying (5). As mentioned earlier, the turbine operating state becomes much more sensitive when ΔP is positive, and as such, the remaining turbines would speed up moving towards the outer threshold (due to the increase in ΔP_i). This process would repeat causing every turbine to cascade towards the outer threshold as depicted in Figure 10.

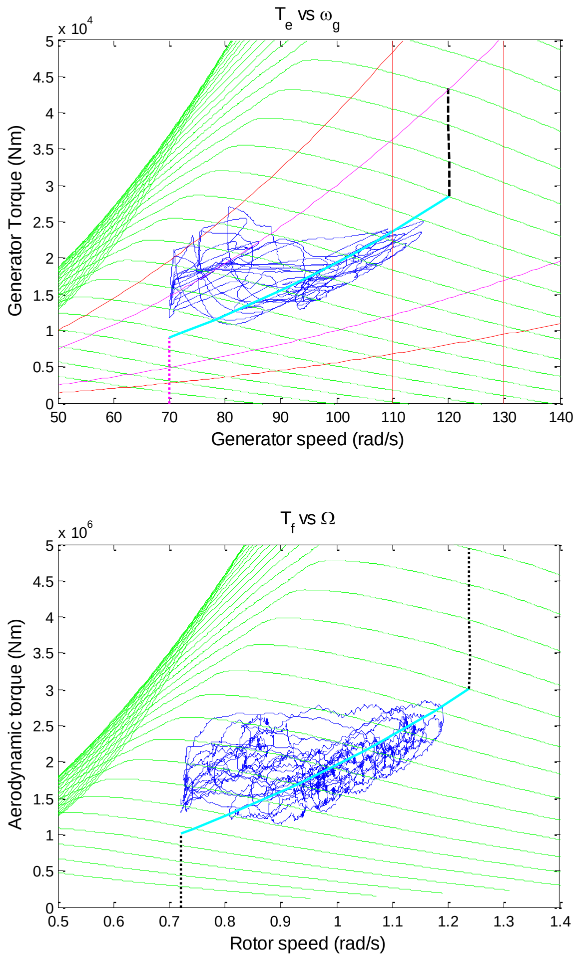

Figure 9: Simulation 2: behaviour of each turbine on the generator torque and generator speed plane (upper subfigure) and the aerodynamic torque and rotor speed plane (lower subfigure).

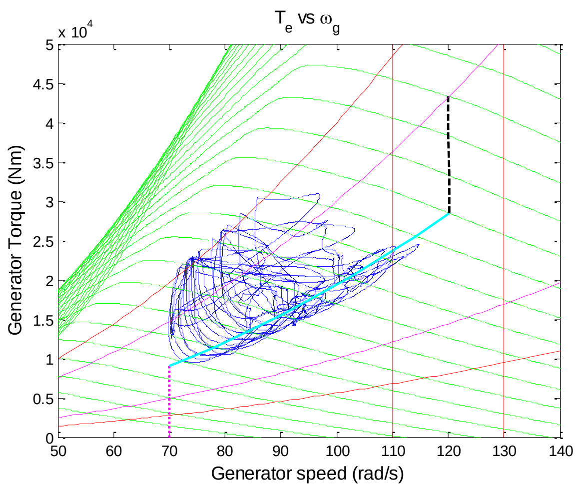

Figure 10: Simulation 2 with (4) and (5): behaviour of each turbine on the generator torque and generator speed plane (upper subfigure).

It consequently leaves a large dip in P as depicted in Figure 11 (just after 270s). As such a large dip would not satisfy the grid opeartion, (6) replaces (4). As a result, when one turbine crosses the outer threshold in the same example, the remaining turbines do not attempt to compensate as depicted in Figure 9 (i.e, ΔP_i of the remaining turbines would not increase), no longer cascading towards the outer threshold. However, (5) is no more satisfied in return, but the undesired dip is removed as depicted in Figure 8 in comparison to Figure 11.

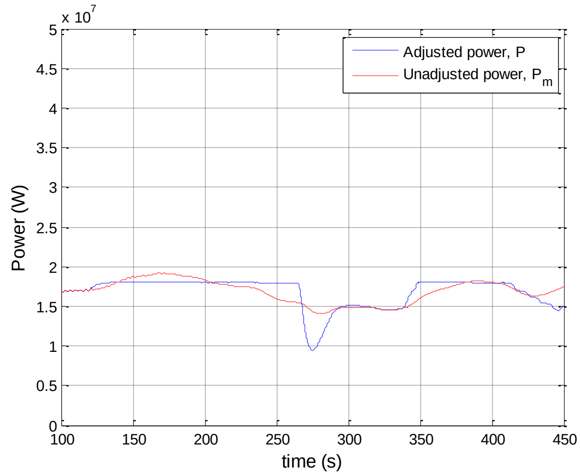

Figure 11: Simulation 2 with (4) and (5): adjusted power vs unadjusted power.

When ΔP is negative such as in Sections 3.1 and 3.3, the turbine operating state is not as sensitive to the change in ΔP_i. Moreover, negative ΔP does not necessatate any compensation afterwards, and therefore, (4) can safely be exploited, hence satisfying (5).

3.3 Simulation 3

In Simulation 3, the wind farm is required to produce a constant power of 25 MW at a mean wind speed of 10 m/s. At this mean wind speed, the controller causes the turbines to switch between the C_{pmax} tracking (mode 2) and the constant speed (mode 3) operations.

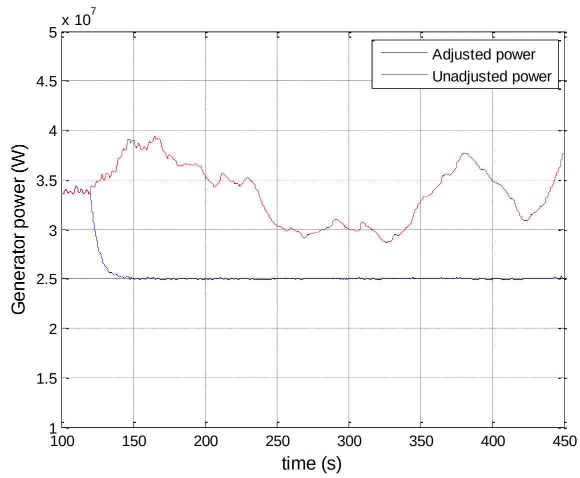

Figure 12: Simulation 3: adjusted power vs unadjusted.

Adjusted power in blue is depicted against unadjusted power in red in Figure 12. The PAC is switched on at 120 s past the transient response. The behaviour of the turbines on the T_e vs ω_g plane and the T_f vs Ω plane is depicted in Figures 13 and 14, respectively. To analyse the simulation results in more detail, attention is drawn to Turbines 1, 2, 6 and 7. Turbines 1 and 2 operate in mode 2 while Turbines 6 and 7 operate in mode 3. The figures depict that Turbines 1 and 2 operate within the thresholds and Turbines 6 and 7 cross the inner threshold. Consequently, Turbines 6 and 7 should be reallocated a reduced power adjustment in comparison to Turbines 1 and 2. Figure 15 (just before 400 s) demonstrates that the reallocation takes place as expected at the switching region.

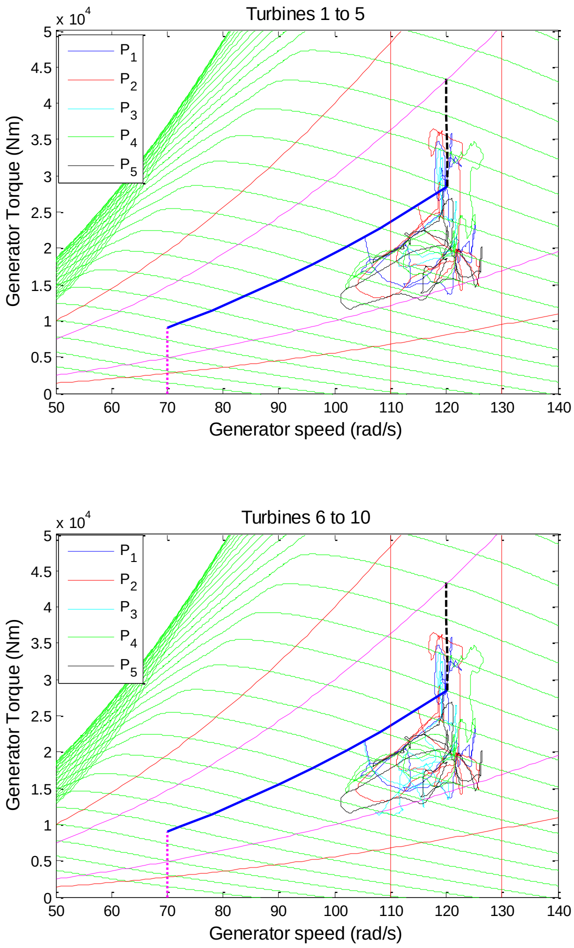

Figure 13: Simulation 3: behaviour of each turbine on the generator torque and generator speed; upper subfigure: turbines 1 to 5, lower subfigure: turbines 6 to 10.

Despite the allocation of reallocation of ΔP to each turbine, adjusted power is still smooth, avoiding the introduction of large transients, discontinuities and steps in the wind farm power output, as depicted (in blue) in Figure 12.

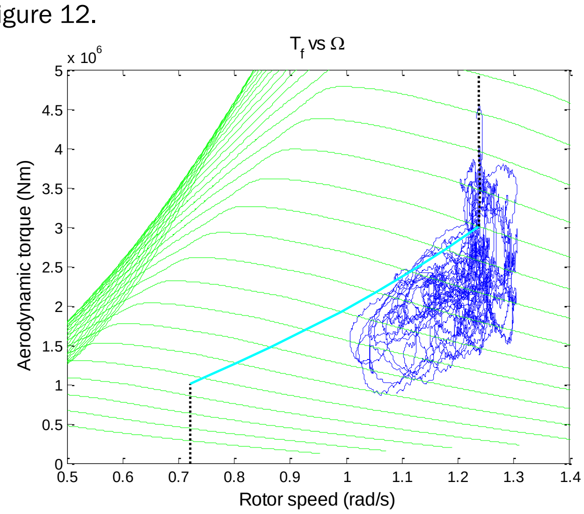

Figure 14: Simulation 3: behaviour of each turbine on the aerodynamic torque and rotor speed plane.

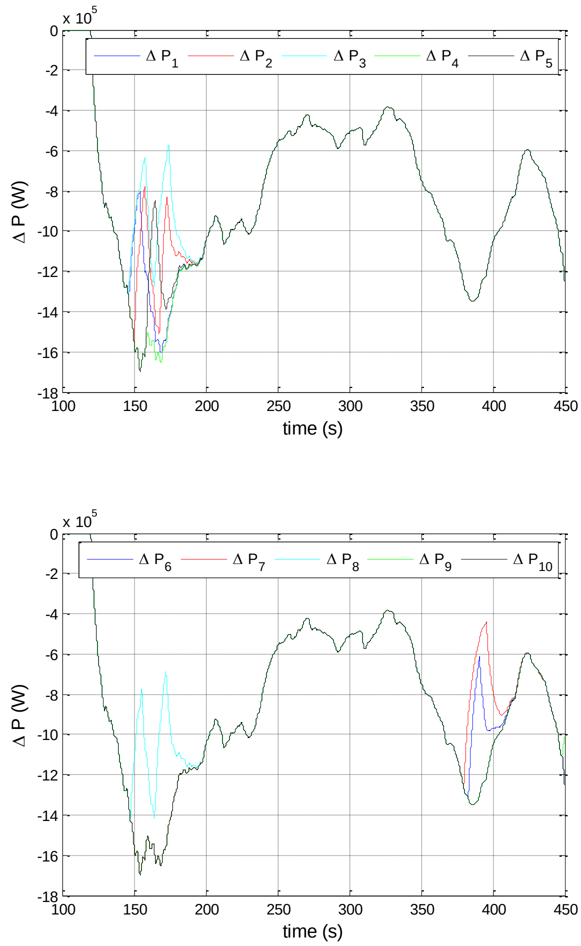

Figure 15: Simulation 3: adjustment in power; upper subfigure: turbines 1 to 5, lower subfigure: turbines 6 to 10.

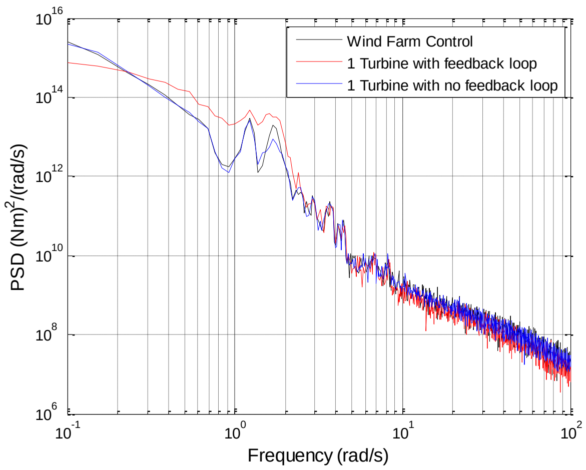

Figure 16: Spectrum of fore-aft tower bending moment (black) in comparison to the situations with (red) and without (blue) a feedback effect.

As reported in Section 2, the change in wind farm power output is determined as the difference between the unadjusted wind farm power output and the wind farm power demand as depicted in Figure 1. This could create a feedback effect and alter the dynamics of the central controllers. However, as the number of turbines in the wind farm increases, the number of turbines that share the adjustments to the wind farm power output (ΔP) increases and the feedback effect decreases. Nonetheless, since there are only 10 turbines in the wind farm, it is important to ensure that the wind farm controller does not create a significant feedback effect.

It is not practical to utilise time-series plots for analysing the feedback effect. The long term effect of the feedback on the structural loads on the tower and blades would not be visible in time-series plots but would clearly be visible in power spectra. Also, the feedback effect could affect the power spectrum at high frequencies but might not appear in time-series plots. Therefore, power spectra are exploited for analysing the feedback effect as follows.

For Simulation 3, the power spectra of fore-aft tower bending moment (TBM), fore-aft blade bending moment (BBM) and side-to-side BBM are depicted in Figures 16, 17 and 18, respectively. The spectra for the situations with (red) and without (blue) a feedback effect are also depicted for comparison purposes. To simulate the situation with a feedback effect, the wind farm controller is applied to a single turbine model, and to simulation the situation without a feedback effect, a constant ΔP is applied with no feedback loop.

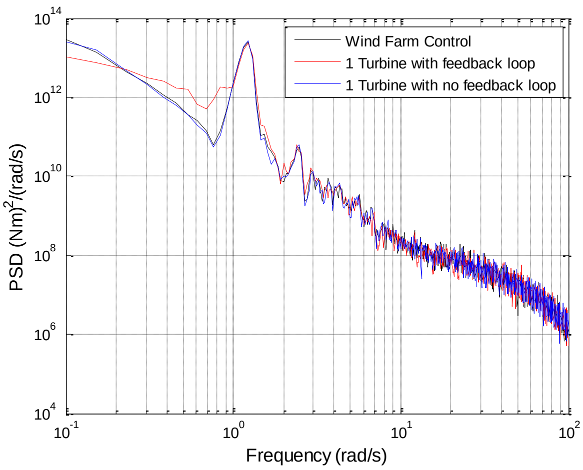

Figure 17: Spectrum of fore-aft blade bending moment (black) in comparison to the situations with (red) and without (blue) a feedback effect.

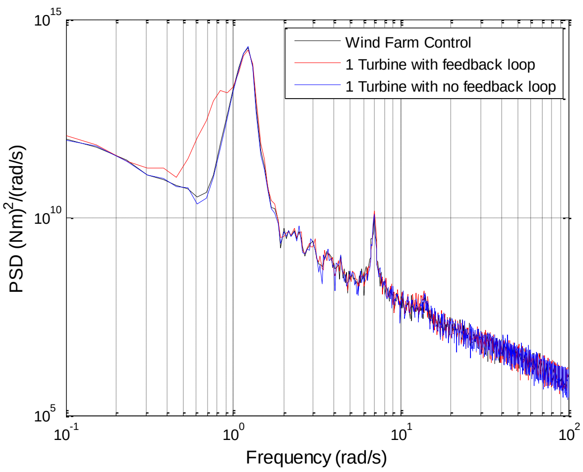

Figure 18: Spectrum of side-to-side blade bending moment (black) in comparison to the situations with (red) and without (blue) a feedback effect.

The results demonstrate that the power spectra for the situation with the wind farm controller and the power spectra for the situation with no feedback loop are analogous. It is, therefore, evident that the wind farm produces a constant power of 25 MW at a mean wind speed of 10 m/s, avoiding creating a significant feedback effect even for a wind farm with only 10 turbines. The feedback effect is even weaker for a wind farm with a larger number of turbines. Almost identical results have been obtained for Simulations 1 and 2.

4 Conclusions

The wind farm controller introduced in this work exploits an existing full envelope controller and the PAC, which has been developed to provide fully flexible operation of each turbine. The wind farm power output meets the wind farm power demand as determined by the grid side operation requirements for the wind farm, taking into account the status and the operating state of each turbine.

The simulation results demonstrate that the wind farm power demand is radidly achieved while keeping each turbine in a safe operating region. The allocation and reallocation of the power adjustments between the turbines takes place in a smooth manner, which avoids the introduction of large transients, discontinuities and steps in the wind farm power output. By curtailing the wind farm power output as opposed to individual turbine power outputs, improved results are attained by allowing those turbines seeing higher wind speeds to compensate for those turbines seeing lower wind speeds. The wind farm controller could also be utilised for increasing the power output as opposed to curtailing. However, the increase in power can only be sustained for a limited time, and the algorithm is modified not to allow those turbines seeing higher wind speeds to compensate for those turbines seeing lower wind speeds for improved results.

The wind farm controller does not cause any significant feedback that could reduce the effectiveness of the turbines' full envelope controllers even for a wind farm with 10 turbines. The feedback effect is even weaker for a wind farm with a larger number of turbines.

Acknowledgement

The authors wish to acknowledge the support of the EPSRC for the Supergen Wind Energy Technologies Consortium, grant number EP/H018662/1.

References

[1] A. P. Chatzopoulos, *Full Envelope Wind Turbine Controller Design for Power Regulation and Tower Load Reduction*, PhD thesis, University of Strathclyde, 2011

[2] A. Stock, "Flexibility of operation", Department of Electronics and Electrical Engineering, University of Strathclyde, SUPERGEN Wind Energy Technologies Consortium Report, 2013.

[3] A. Stock and W. E. Leithead, "Providing grid frequency support using variable speed wind turbines with augmented control" in proceedings of European Wind Energy Association (EWEA) Conference, Copenhagen, 2012.

[4] T. Burton, D. Sharpe, N. Jenkins, E. Bossanyi, *Wind Energy Handbook*, John Wiley & Sons, Ltd.

[5] F. D. Bianchi, H. Battista and R. J. Mantz, *Wind Turbine Control Systems: Principles, Modelling and Gain Scheduling Design*, Springer, 2006.

[6] I. Munteanu, A. I. Bratcu, N. A. Cutululis and E. Ceanga, *Optimal Control of Wind Energy Systems: Towards a Global Approach,* Springer, 2007.

[7] W. E. Leithead, "Effective wind speed models for simple wind turbine simulations" in proceedings of 14th British Wind Energy Association (BWEA) Conference, Nottingham, 1992.

[8] W. E. Leithead and B. Connor, "Control of variable speed wind turbines: design task" International Journal of Control, vol. 13, pp. 1189–1212, 2000.